Two proofreading steps amplify the accuracy of genetic code translation

Ka-Weng Ieong[a], Ülkü Uzun[a,1], Maria Selmer[a], and Måns Ehrenberg[a,2]

[a]Department of Cell and Molecular Biology, Uppsala University, Uppsala 75124, Sweden

Edited by Ada Yonath, Weizmann Institute of Science, Rehovot, Israel, and approved October 12, 2016 (received for review July 4, 2016)

Aminoacyl-tRNAs (aa-tRNAs) are selected by the messenger RNA programmed ribosome in ternary complex with elongation factor Tu (EF-Tu) and GTP and then, again, in a proofreading step after GTP hydrolysis on EF-Tu. We use tRNA mutants with different affinities for EF-Tu to demonstrate that proofreading of aa-tRNAs occurs in two consecutive steps. First, aa-tRNAs in ternary complex with EF-Tu·GDP are selected in a step where the accuracy increases linearly with increasing aa-tRNA affinity to EF-Tu. Then, following dissociation of EF-Tu·GDP from the ribosome, the accuracy is further increased in a second and apparently EF-Tu–independent step. Our findings identify the molecular basis of proofreading in bacteria, highlight the pivotal role of EF-Tu for fast and accurate protein synthesis, and illustrate the importance of multistep substrate selection in intracellular processing of genetic information.

ribosome | error correction | fidelity | EF-Tu | ternary complex

We have found that the bacterial ribosome uses two proofreading steps following initial selection of transfer RNAs (tRNAs) to maintain high accuracy of translation of the genetic code. This means that there are three selection steps for codon recognition by aa-tRNAs. First, there is initial codon selection by aa-tRNA in ternary complex with elongation factor Tu (EF-Tu) and GTP. Second, there is proofreading of aa-tRNA in ternary complex with EF-Tu and GDP. Third, there is proofreading of aa-tRNA in an EF-Tu–independent manner, presumably after dissociation of EF-Tu·GDP from the ribosome (Fig. 1). Seven decades ago, Linus Pauling suggested that the precision by which proteins can choose between cognate and near-cognate substrates of similar structures is greatly limited, and he predicted high amino acid substitution frequency in intracellular protein synthesis (1). However, experiments by Robert Loftfield with rabbit reticulocyte hemoglobin demonstrated an error frequency much lower than Pauling's prediction (2). One way to resolve this apparent paradox was offered by the principle of proofreading, first formulated by Hopfield (3) and Ninio (4). By this principle, the very same standard free energy difference, $\Delta\Delta G^0$, between enzyme-bound noncognate and cognate substrate can be used in both initial selection (I) and subsequent proofreading selection (F) to boost the total accuracy ($A = I \times F$) of selective enzymes above their single-step selection limits. Accuracy amplification by proofreading requires substrate discarding to be driven by a chemical potential decrease from the entering of a substrate to its exit along the proofreading path. One way to implement such a drop in chemical potential is to couple the discarding of substrates by proofreading to hydrolysis of GTP or ATP at high chemical potential to the low chemical potential of their hydrolytic products (5, 6).

Proofreading was first discovered for the IleRS enzyme, which aminoacylates $tRNA^{Ile}$ to cognate Ile-$tRNA^{Ile}$ and efficiently suppresses near-cognate Val-$tRNA^{Ile}$ formation by discarding valine through ATP hydrolysis-driven proofreading (7). Soon thereafter, GTP-driven proofreading of codon reading by aa-tRNAs on the mRNA-translating ribosome was discovered (8, 9) and subsequently subjected to extensive research (10–13). Although it was early recognized that multistep proofreading confers higher accuracy and kinetic efficiency to substrate-selective, enzyme-catalyzed reactions than single-step proofreading (5, 14, 15), it has been taken for granted that there is but a single proofreading step in tRNA selection by the translating ribosome (16). Here, we present data showing that the proofreading factor (F), by which the accuracy (A) is amplified from its initial selection value (I) by aa-tRNA in ternary complex with EF-Tu and GTP, increases linearly with increasing association equilibrium constant, K_A, for aa-tRNA binding to EF-Tu. We suggest the cause of this linear increase to be the activity of a first proofreading step, in which aa-tRNA is discarded in complex with EF-Tu and GDP whereas the forward reaction is release of EF-Tu·GDP. In the limit of zero affinity between aa-tRNA and EF-Tu, where the first proofreading step is expected to be completely turned off, we observe a remaining accuracy amplification by proofreading. This amplification, we suggest, comes from the activity of a second proofreading step, involving aa-tRNA only (Fig. 1). We use the present results to discuss the molecular basis for proofreading of aminoacyl-tRNAs, which, until now, has remained obscure (17). We suggest that multistep proofreading in genetic code translation has evolved to neutralize potential error hot spots originating in error-prone initial selection of aa-tRNA in ternary complex with EF-Tu and GTP (18, 19). Recent cryo-EM data of ribosomes from live human cells show two states of ribosome-bound preaccommodated aa-tRNA, one with aa-tRNA in complex with the EF-Tu homolog eEF1α in the GDP form, the other with only aa-tRNA after release of eEF1α·GDP (20). With support from these cryo-EM data in conjunction with the present findings, we suggest that two-step proofreading mechanisms are at work not only in bacteria but also in eukaryotes and, perhaps, in all three kingdoms of life.

Significance

We have discovered that two proofreading steps amplify the accuracy of genetic code reading, not one step, as hitherto believed. We have characterized the molecular basis of each one of these steps, paving the way for structural analysis in conjunction with structure-based standard free energy computations. Our work highlights the essential role of elongation factor Tu for accurate genetic code translation in both initial codon selection and proofreading. Our results have implications for the evolution of efficient and accurate genetic code reading through multistep proofreading, which attenuates the otherwise harmful effects of the obligatory tradeoff between efficiency and accuracy in substrate selection by enzymes.

Author contributions: K.-W.I. and M.E. designed research; K.-W.I. and Ü.U. performed research; M.S. performed structural analysis; K.-W.I. and M.E. analyzed data; and K.-W.I. and M.E. wrote the paper.

The authors declare no conflict of interest.

This article is a PNAS Direct Submission.

Freely available online through the PNAS open access option.

[1]Present address: Department of Biochemistry, University of Oxford, Oxford OX1 3QU, United Kingdom.

[2]To whom correspondence should be addressed. Email: ehrenberg@xray.bmc.uu.se.

This article contains supporting information online at www.pnas.org/lookup/suppl/doi:10.1073/pnas.1610917113/-/DCSupplemental.

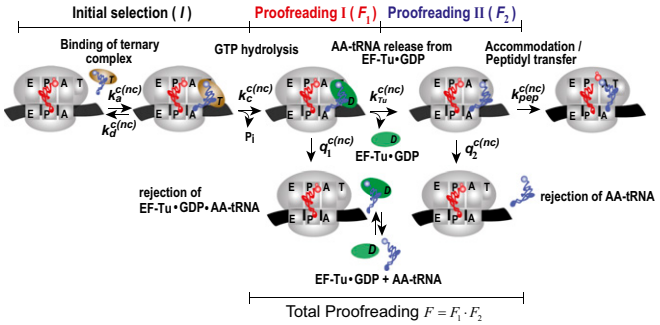

Fig. 1. Proposed schematic of tRNA selection in bacterial protein synthesis. A ternary complex with aa-tRNA and EF-Tu·GTP binds to A/T state of the pre-translocation ribosome with association rate constant k_a. Then, the ternary complex dissociates with rate constant k_d or GTP is hydrolyzed with rate constant k_c, leading to ribosome-bound ternary complex EF-Tu·GDP·aa-tRNA, which dissociates with rate constant q_1, or EF-Tu·GDP dissociates with rate constant k_{Tu}, leading to an aa-tRNA–bound preaccommodation state of the ribosome. From this state, aa-tRNA dissociates with rate constant q_2 or accommodates into the A site with rate constant k_{pep}. There are three selection steps in this scheme: Near-cognate tRNA can be rejected during initial selection (*I*), first proofreading step (F_1), and second proofreading step (F_2). Notations ^{c} and ^{nc} in rate constants stand for cognate and noncognate reaction, respectively.

Results

Mg^{2+} Concentration Dependence of Proofreading Factors in Genetic Code Translation. The concentration of free Mg^{2+} ions affects the accuracy of initial codon selection, *I*, in mRNA translation by decreasing the rate constant for dissociation of ternary complex from its precodon recognition state (21, 22). Here, we first studied the effect of Mg^{2+} concentration on the proofreading parameter, *F*, by which Glu-tRNA^{Glu} favors its cognate GAA codon in relation to its near-cognate GAU, GGA and GAC codons. For this study, we estimated the k_{cat}/K_m values for GTP hydrolysis on a Glu-tRNA^{Glu}–containing ternary complex reading GAA, GAU (Fig. 2*A*), GGA, and GAC in the A site of ribosomes with initiator fMet-tRNA^{fMet} in the P site. In each case, the ratio between cognate and near-cognate k_{cat}/K_m values estimated the initial selection accuracy, *I* (22). We also determined the k_{cat}/K_m values for fMet-Glu-tRNA^{Glu} formation in each one of these four cases and thereby obtained the total accuracy, $A = I \times F$, of peptide bond formation with Glu-tRNA^{Glu} reading its cognate GAA codon versus the near-cognate GAU (Fig. 2*B*), GGA, and GAC codons. Then, the proofreading parameter *F* was, in each case, estimated as the *A*/*I* ratio at different Mg^{2+}concentrations (Fig. 2 *D* and *E*). We also estimated the accuracy, A_{nf}, where $_{nf}$ stands for "no factor," by which fMet-Glu-tRNA^{Glu} formation was favored by the cognate GAA codon in relation to the near-cognate GAU (Fig. 2*C*), GGA, and GAC codons in the absence of the translation factor EF-Tu (Scheme S1). For this work, we estimated k_{cat}/K_m values for factor-free codon reading by Glu-tRNA^{Glu} under conditions identical to those under which the *F* values for the EF-Tu–facilitated reactions were obtained.

The proofreading parameter *F* decreases sharply with increasing free Mg^{2+} concentration in the low concentration range (Fig. 2 *D* and *E*). At the same time, the factor-free codon selection accuracy varies much more gradually in the low Mg^{2+} concentration range, bringing the initially higher proofreading factor, *F*, closer to factor-free accuracy, A_{nf} (Fig. 2*F*). Inspired by these preliminary observations, we hypothesized that EF-Tu might affect the proofreading factor, *F*, in a first step and that there is a second, apparently EF-Tu–independent, proofreading step (Fig. 1). The simplistic idea was that, because the accuracy of initial selection of codons by aa-tRNA in ternary complex with EF-Tu·GTP decreases sharply with increasing Mg^{2+} concentration (22), such a high Mg^{2+} sensitivity could be typical also of a first proofreading step in which aa-tRNA in ternary complex with EF-Tu·GDP is discarded. Furthermore, because the accuracy of factor-free codon selection has comparatively low sensitivity to Mg^{2+} concentration (Fig. 2*F*), such a low Mg^{2+} sensitivity could be typical of a second proofreading step after dissociation of EF-Tu·GDP from the ribosome. We decided to subject this hypothesis to stringent testing in a series of experiments that were inspired by the observation that the choice of base pairs in the T stem of any tRNA strongly affects its affinity to EF-Tu · GTP (23). For these experiments, we first developed a kinetic model for two-step proofreading in ribosomal protein synthesis in bacteria (Fig. 1) as described in *Mechanistic Model of a Two-Step Proofreading Mechanism*.

Mechanistic Model of a Two-Step Proofreading Mechanism in Bacterial Protein Synthesis. We designed a kinetic model for codon selection in an initial step, before GTP hydrolysis on EF-Tu, followed by accuracy amplification in two proofreading steps (Fig. 1). Initial codon selection by aa-tRNA in ternary complex with EF-Tu·GTP is followed by a first proofreading step in which aa-tRNA in ternary complex with EF-Tu·GDP is discarded or, alternatively, EF-Tu·GDP dissociates from the ribosome-bound aa-tRNA. In a second proofreading step, aa-tRNA is discarded in an EF-Tu–independent manner or, alternatively, accommodated in the A site. The first proofreading step contributes by the factor F_1 and the second contributes by the factor F_2 to the overall proofreading factor *F*, so that $F = F_1 \cdot F_2$. Accordingly, the overall accuracy, *A*, is given by $A = I \cdot F = I \cdot F_1 \cdot F_2$.

The model predicts that, as long as the current accuracy amplification of the first proofreading step is much smaller than its maximal value, d_{F1}, then F_1 is a linear function of the inverse, $1/k_{Tu}$, of the rate constant for dissociation of EF-Tu·GDP from its ribosome-bound complex with aa-tRNA (Fig. 1) (*SI Three-Step Codon Selection*). In the limit of small $1/k_{Tu}$, F_1 reaches its smallest value, $F_1 = 1$, and the total proofreading factor *F* is equal to F_2. In the absence of an EF-Tu–dependent first proofreading step, the total proofreading *F* would always be equal to F_2 and would not be expected to vary with varying binding affinity of aa-tRNA to EF-Tu. In the absence of a second proofreading step, *F* would always be equal to F_1 and thus equal to 1 in the limit of small $1/k_{Tu}$. In the limit of high $1/k_{Tu}$, F_1 would be close to its maximal value, d_{F1}, at the cost of huge excess hydrolysis of GTP per cognate peptide bond (see *SI Three-Step Codon Selection*). To test the model prediction of a linear relation between the proofreading amplification *F* and $1/k_{Tu}$, we took advantage of the findings by Uhlenbeck and colleagues that base pairs in the T stem of tRNAs greatly affect their affinity, K_A (per molar), to EF-Tu in the GTP form (24). We note that K_A is the ratio between the rate constants for formation and dissolution of the ternary complex between EF-Tu·GTP and aa-tRNA off the ribosome. The experimental determination of K_A and the relation between k_{Tu} and K_A are discussed in *Tuning the Affinity Between aa-tRNA and EF-Tu·GTP*.

Tuning the Affinity Between aa-tRNA and EF-Tu·GTP by tRNA T-Stem Engineering. We used T7 RNA polymerase transcription of DNA oligos for in vitro production of five T-stem mutants of tRNA^{Glu}, WT, strong (T1 and T2), and weak (W1 and W2) variants, and four of tRNA^{Phe}, WT, strong (T1 and T2), and weak (W1) variants (Fig. 3), and we estimated association equilibrium constants, K_A, for binding of their aminoacylated variants to free EF-Tu·GTP. The K_A values were obtained from experiments in which the time dependence of dipeptide formation (fMet-Glu or fMet-Phe) was monitored at constant Glu-tRNA^{Glu} or Phe-tRNA^{Phe} concentration and varying EF-Tu concentration (25). Dipeptide formation from both Glu-tRNA^{Glu} and Phe-tRNA^{Phe}–containing ternary complex is biphasic as illustrated for the wild-type tRNAs in Fig. S1 *A* and *C*, respectively. The fast phase reflects peptide bond formation from preformed ternary complex, and the slow phase reflects ternary complex formation from free EF-Tu and aa-tRNA (25). Accordingly, the K_A value could, in each case, be estimated from the EF-Tu concentration dependence of the fast-phase fraction (Fig. S1 *B* and *D* and *SI Materials and Methods*). The rate constant for the fast phase,

BIOCHEMISTRY

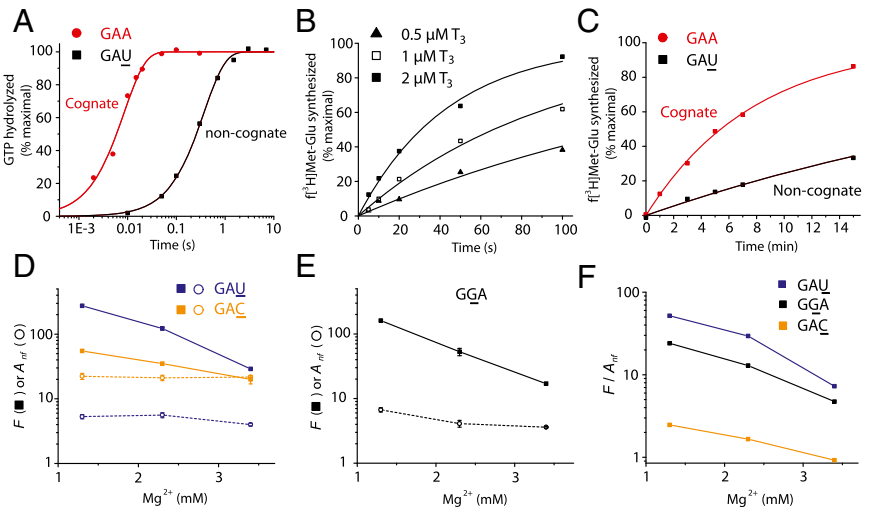

Fig. 2. The proofreading factor of ternary complex selection converges to the accuracy of tRNA selection without EF-Tu at high Mg^{2+} condition. (*A*) Measurements of GTP hydrolysis for native Glu-tRNA^{Glu} ternary complex (T_3; 0.5 μM) binding to 70S initiation complex (IC; 2 μM) programmed with a cognate (GAA, curve in red) or near-cognate (GAU, curve in black) codon in the A site. (*B*) Kinetics of dipeptide formation from Glu-tRNA^{Glu} reading GAU with varying T_3 concentration. (*C*) Kinetics of EF-Tu–free dipeptide formation from Glu-tRNA^{Glu} reading GAA or GAU with 3 μM tRNA (Scheme S1). (*D*) [Mg^{2+}] dependence of the proofreading factor, *F* (filled squares), for codon selection by Glu-tRNA^{Glu} in ternary complex with EF-Tu·GTP and of the accuracy (A_{nf}, opened circles) for EF-Tu–free codon selection by Glu-tRNA^{Glu}. (*E*) Similar to *D*, Glu-tRNA^{Glu} reading GGA. (*F*) [Mg^{2+}] dependence of the F/A_{nf} ratio for Glu-tRNA^{Glu} reading cognate GAA versus near-cognate GAU (blue), GGA (black), and GAC (yellow). Experiments in *A*–*C* were performed in buffer containing 2.3 mM free Mg^{2+}. Kinetic data in *A*–*C* are representative of at least two independent experiments and are fitted to a single exponential model (see *SI Materials and Methods*). Data in *D* and *E* represent weighted averages from at least two experiments ± propagated SD.

k_{dip}, defined as the inverse of the total reaction times for all steps leading from free ternary complex and ribosome to peptide bond formation (25, 26), is for all tRNA mutants displayed in Table S1. It is seen that the aa-tRNA mutants display a 10-fold and 30-fold K_A variation in the tRNA^{Glu} and tRNA^{Phe} cases, respectively (Fig. 3, Fig. S1, and Table S1). There is also some k_{dip} variation among the tRNA mutants (Table S1). In the tRNA^{Phe} case, the similar k_{dip} values in the WT and W1 cases (Table S1) are much smaller than the maximal rate of peptide bond formation (26) and must therefore reflect similar k_{cat}/K_m values for the reaction. We suggest that the significantly smaller k_{dip} values for the "strong" T1 and T2 variants in relation to the WT and W1 variants reflect slow release of EF-Tu·GDP from the ribosome, as previously proposed (23). In the tRNA^{Glu} case, the k_{dip} value is similar among the WT, T1, and T2 variants, reflecting similar k_{cat}/K_m values for peptide bond formation. For the very weak W1 and W2 variants, the k_{dip} values are significantly smaller than for the WT, T1, and T2 variants (Table S1). This reflects, we suggest, reduced catalytic rate of GTPase activation that, under these conditions, decreases the k_{cat}/K_m values. We note that the existence of different k_{dip} values for the mutants of one isoaccepting tRNA does not in any way distort the K_A estimates but shows that the mutations may, in some cases, have effects additional to K_A-value tuning. We note that, in the tRNA^{Glu} case, K_A is larger for WT tRNA than for the nominally strong T1 and T2 variants (Table S1). This apparent anomaly of nomenclature is explained by the observation that WT tRNA^{Glu} has the highest affinity to EF-Tu·GTP among the *Escherichia coli* tRNAs (27). The implication here is that any mutation is expected to result in lower than WT affinity to the tRNA isoacceptor.

The K_A values determined here (Table S1) refer to the binding of aa-tRNA to EF-Tu·GTP off the ribosome. Relevant for the testing of the model in Fig. 1 is, however, the rate constant for dissociation of EF-Tu·GDP from ribosome-bound aa-tRNA (k_{Tu}). We note that the dramatic structural change of EF-Tu from the GTP to GDP form is compatible with preserved interaction between the T stem of aa-tRNA and EF-Tu off the ribosome (Fig. 4*A*). Furthermore, the shift in ternary complex conformation depicted in Fig. 4*A* could be modeled on the ribosome without any clashes (Fig. 4*B*). Thus, in the GDP form, the G domain would lose its interactions with the acceptor stem of tRNA as well as with the sarcin–ricin loop of 23S RNA, domain III of EF-Tu would contact the T stem of tRNA, and domain II would possibly contact the acceptor stem, and, if the tRNA remains in the same position, the h5 and h15 region of 16S rRNA. This finding suggests that ratios between association equilibrium constants for aa-tRNA T-stem mutants binding to free EF-Tu·GTP (K_A), ribosome-bound EF-Tu·GTP and ribosome-bound EF-Tu·GDP are similar, although their absolute values are expected to be very different. It is, finally, likely that the major effect of the T-stem variations is on the rate constant for dissociation of EF-Tu from aa-tRNA, so that estimated ratios between K_A values predict the inverse ratios of the corresponding rate constants for dissociation of EF-Tu·GDP from ribosome-bound aa-tRNA, k_{Tu} (Fig. 1). In *Proofreading Factor* F *Increases Linearly with Association Equilibrium Constant* (K_A) *for aa-tRNA Binding to EF-Tu·GTP*, we provide experimental proof that the overall proofreading factor *F* increases linearly with increasing K_A in six cases of near-cognate misreading by WT and mutated variants of Glu-tRNA^{Glu} and Phe-tRNA^{Phe} (Fig. 5).

Proofreading Factor *F* Increases Linearly with Association Equilibrium Constant (K_A) for aa-tRNA Binding to EF-Tu·GTP. We estimated the overall proofreading factor *F* for the five variants of tRNA^{Glu} misreading GAU, GGA, and GAC and the four variants of tRNA^{Phe} misreading CUC, UCC, and UUA. For this work, we determined the initial codon selection accuracy, *I* (Fig. S2 *A* and *D* as examples for WT tRNA^{Glu} and tRNA^{Phe}, respectively, and Tables S2 and S3), the total accuracy of peptide bond formation, *A* (Fig. S2 *B* and *E*), and the total proofreading factor, $F = A/I$ (Tables S2 and S3). We plotted *F* versus K_A for Glu-tRNA^{Glu} misreading GAU (Fig. 5*A*), GGA (Fig. 5*B*), and GAC (Fig. 5*C*) and for tRNA^{Phe} misreading CUC (Fig. 5*D*), UCC (Fig. 5*E*), and UUA (Fig. 5*F*). For comparison, we also measured corresponding accuracy values of factor-free codon selection (A_{nf}) (Fig. S2 *C* and *F* as examples for WT tRNA^{Glu} and tRNA^{Phe}, respectively, and Table S4), and those were plotted versus K_A for each one of these tRNA^{Glu} and tRNA^{Phe} variants reading their near-cognate codons. In all cases (Fig. 5), the *F* parameter increased linearly with increasing K_A value, corroborating the hypothesis that there is a first proofreading step with accuracy amplification, F_1, in which aa-tRNA can be discarded in ternary complex with EF-Tu·GDP. Furthermore, the linear dependence of F_1 on K_A and, by hypothesis, $1/k_{Tu}$, shows that, in these experiments, the proofreading accuracy was far below its maximal value, d_{F1} (see *SI Three-Step Codon Selection*). The intercepts with the *y* axis at zero K_A value reveal proofreading factors F_2 between 10 and 50. The straightforward interpretation of these results is that the intercepts reflect the accuracy contribution, F_2, from a second, EF-Tu–independent proofreading step. Further analysis of the correspondence between association equilibrium constant K_A and dissociation time $1/k_{Tu}$ (Fig. 1; see *SI More Detailed Model of the First Proofreading Step*) shows that sequential dissociation

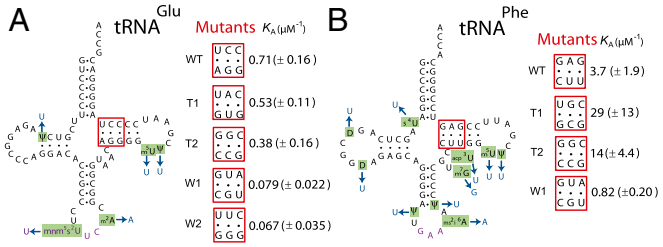

Fig. 3. Engineered tRNA mutants with altered EF-Tu affinities. (*A*) The $tRNA^{Glu}$ and (*B*) $tRNA^{Phe}$ mutants with T-stem mutated sequences (positions 51 to 53 and 61 to 63, shown in red boxes). T-stem sequences of WT and different mutants with their corresponding K_A values for EF-Tu binding are shown. (K_A values are in per micromolars; see also Fig. S1 and Table S1. Data represent weighted averages from at least two independent experiments ± propagated SD.) All tRNAs (WT and mutants) were unmodified and based on native *E. coli* (*A*) $tRNA^{Glu}$ or (*B*) $tRNA^{Phe}$ (black with purple anticodon; tRNA modifications are in green) with changes in blue.

from the ribosome of EF-Tu·GDP followed by aa-tRNA at insignificant mutual affinity leads to a y axis intercept of F in Fig. 5 reflecting the accuracy amplification, F_2, of a subsequent proofreading step and not a putative, residual activity of the EF-Tu–dependent, first proofreading step. Inspection of the ribosome structure in Fig. 4 with aa-tRNA and EF-Tu·GDP shows that the two macromolecules must either dissociate together or with EF-Tu·GDP leaving first followed by dissociation of aa-tRNA, even in the case when EF-Tu·GDP has significant affinity to the ribosome itself. This means that F_1 can be written as (see *SI Relationship Between Proofreading and EF-Tu Affinity to aa-tRNA*)

$$F_1 = \frac{1 + c_p K_A d_{F1}}{1 + c_p K_A},$$

where c_p is a proportionality constant with unit micromolars, K_A is the association constant with unit of per micromolar and d_{F1} is the unitless maximal accuracy of the EF-Tu·GDP–dependent step. From these experiments, the analysis of available structures (Fig. 4) and the analysis in *SI Relationship Between Proofreading and EF-Tu Affinity to aa-tRNA* and *SI More Detailed Model of the First Proofreading Step*, we suggest that the first, EF-Tu–dependent proofreading step with accuracy amplification, F_1, is followed by a second, EF-Tu–independent proofreading step with accuracy F_2 that can be estimated from the y axis intercepts in Fig. 5 (*Discussion*). Accordingly, the total accuracy amplification F is given by $F = F_1 \cdot F_2$, where F_1, F_2, and F are in the ranges 1 to 8, 10 to 50, and 10 to 250, respectively. We note that the factor-free accuracy of codon selection, A_{nf}, is remarkably similar to the accuracy amplification, F_2, in the second proofreading step (compare the proofreading and A_{nf} intercepts in Fig. 5). To assess the significance of this similarity, we estimated the average value of F_2/A_{nf} over all intercepts in Fig. 5 as 0.98 ± 0.08 (see *SI Materials and Methods*). This high-precision value close to 1 suggests strongly correlated values of F_2 and A_{nf} (see *SI Factor-Free Codon Selection by aa-tRNA* and *Discussion*).

Discussion

Major Conclusion: Two Proofreading Steps in Bacterial Protein Synthesis. We found that proofreading amplification of the accuracy of codon reading by aa-tRNAs, F, increases linearly with the affinity (K_A value) of aa-tRNAs to EF-Tu·GTP (Fig. 5) when K_A is varied by T-stem mutations (23). From this finding, we propose that EF-Tu plays a fundamental role not only in initial codon selection by ternary complex in the GTP conformation but also in the rechecking of the initial codon choice in a proofreading step following GTP hydrolysis on EF-Tu, Pi release, and conformational change of the factor (Fig. 1). By this mechanism, GTP hydrolysis on ribosome-bound EF-Tu first leads to a ribosome complex with aa-tRNA, EF-Tu·GDP, and inorganic phosphate, Pi, in which aa-tRNA is strongly bound to EF-Tu (16). After rapid release of Pi, EF-Tu changes conformation from the GTP to the GDP form. This leads to a ribosome complex with aa-tRNA·EF-Tu·GDP, in which aa-tRNA is weakly bound to EF-Tu. Our proposal is now that the discard reaction of the K_A-dependent proofreading step is dissociation of aa-tRNA·EF-Tu·GDP and that the forward reaction is dissociation of EF-Tu·GDP from ribosome-bound aa-tRNA (Fig. 1). In favor of this proposal, we note that the interaction between the T-stem base pairs and aa-tRNA can be preserved as EF-Tu changes conformation in response to GTP hydrolysis and Pi release (Fig. 4*A*) and, furthermore, that the transition of ternary complex from its GTP to GDP conformation can occur on the ribosome without sterical clashes (Fig. 4*B*). From this finding, we suggest, from an elementary thermodynamic consideration, that relative changes in the association constant, K_A, in response to T-stem mutations predict the relative changes in the inverse, $1/k_{Tu}$, of the rate constant for dissociation of EF-Tu·GDP from ribosome-bound aa-tRNA (Fig. 1). This relation between K_A and $1/k_{Tu}$ readily explains the experimentally observed linear relation between F and K_A in terms of an EF-Tu·GDP–dependent proofreading step by which the accuracy of codon selection of aa-tRNAs is amplified by a factor F_1 (*Results* and *SI Relationship Between Proofreading and EF-Tu Affinity to aa-tRNA*).

We observe that the straight lines connecting the proofreading factor, F, with K_A intercept the y axis at values significantly larger than 1 (Fig. 5) and note that these intercepts are readily explained in terms of a second, K_A-independent, proofreading step by which the accuracy of codon selection is amplified by a factor F_2. We suggest that the latter step has EF-Tu–independent release of aa-tRNA as its discard reaction and accommodation of aa-tRNA in the A site as its forward reaction. Could, then, an alternative model with dissociation of aa-tRNA in complex with EF-Tu·GDP·Pi as discard reaction account for the present experimental results?

According to this model, aa-tRNA would be discarded in complex with EF-Tu·GDP·Pi after GTP hydrolysis but before Pi release and conformational change of EF-Tu (16). Due to high affinity of aa-tRNA to EF-Tu before the conformational change of the factor, the forward rate constant in such a step would not be dissociation of

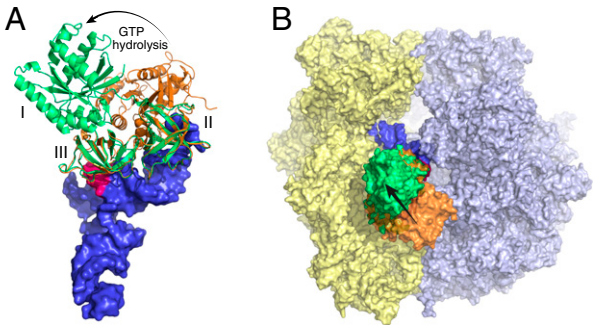

Fig. 4. Interaction between EF-Tu and the T-stem base pairs of aa-tRNA in ternary complex before and after GTP hydrolysis on the ribosome. (*A*) Overlay of EF-Tu·GDP [green, Protein Data Bank (PDB) 1tui (35)] based on domains II and III onto EF-Tu·GDPCP (orange) in complex with Trp-$tRNA^{Trp}$ G24A (blue) bound to the 70S ribosome from *Thermus thermophilus* [PDB 4v5l (36)]. The tRNA base pairs 51 to 63, 52 to 62, and 53 to 61 in the T stem are highlighted in hot pink. Domains II and III of EF-Tu·GDP superpose onto the same domains from EF-Tu·GDPCP with a root-mean-square deviation of 0.79 Å over 189 C_α atoms. (*B*) The complex of EF-Tu·GDP with aminoacyl-tRNA is sterically compatible with ribosome binding; 30S is shown in light yellow, and 50S is shown in light blue. The conformational change upon GTP hydrolysis is indicated by an arrow. Superpositioning was done using the LSQ commands in O (37). The images were prepared using Pymol version 1.8 (Schrödinger, LLC).

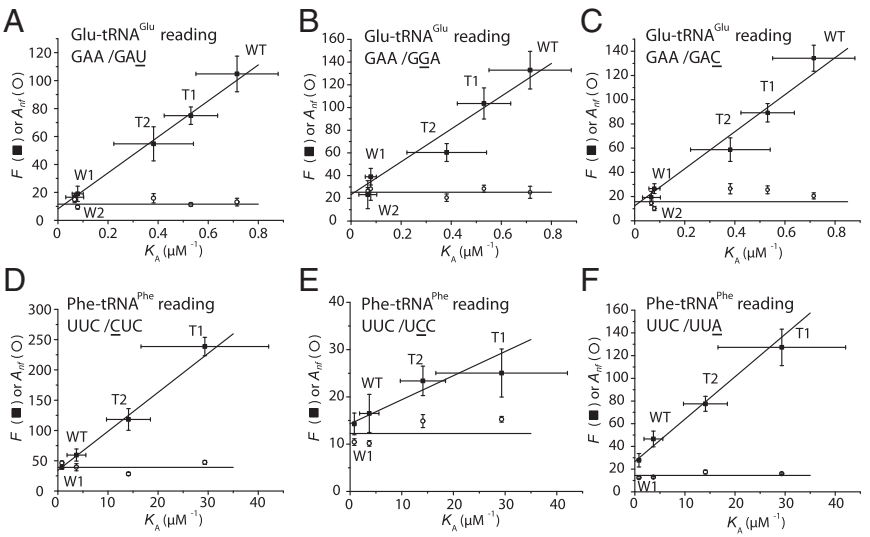

Fig. 5. Proofreading factors, F, for codon selection by ternary complex increase linearly with increasing aa-tRNA affinity to EF-Tu at unaltered accuracy (A_{nf}) of EF-Tu–free codon selection. F and A_{nf} from different tRNA mutants are plotted against the tRNA affinities to EF-Tu (K_A). Measurements are shown for Glu-tRNA^{Glu} mutants misreading (*A*) GAU, (*B*) GGA, and (*C*) GAC and Phe-tRNA^{Phe} mutants misreading (*D*) CUC, (*E*) UCC, and (*F*) UUA by their ternary complexes (F, ■) or aa-tRNAs only (A_{nf}, ○). In each case, linear regression was used to obtain maximum likelihood estimates of the y axis intercepts F_2 and A_{nf} as (*A*) 8.2 ± 5.0 and 12 ± 0.8, (*B*) 23 ± 8 and 25 ± 2, (*C*) 12 ± 5 and 16 ± 1, (*D*) 34 ± 4 and 39 ± 2, (*E*) 14 ± 2 and 12 ± 0.3, and (*F*) 27 ± 6 and 14 ± 0.4. Errors of F_2 and A_{nf} estimates represent SD from data fitting procedure (see *SI Materials and Methods*). Data in the plots represent weighted averages from at least two independent experiments ± propagated SD in both dimensions. Measurements were performed in polymix buffer containing 2.3 mM free Mg^{2+}.

EF-Tu·GDP·Pi from the ribosome-bound aa-tRNA but Pi release and conformational change of the factor (16). Therefore, such a proofreading step would not be expected to display the linear dependence of the proofreading factor F on the affinity parameter K_A as predicted by our model (Fig. 1) and observed by experiment (Fig. 5). Then, could there be two EF-Tu–dependent proofreading steps, where aa-tRNA is discarded with EF-Tu·GDP·Pi in the first step and, after Pi release and conformational change of the factor, with EF-Tu·GDP in the second step? Although we cannot exclude this possibility, the latter model is made less attractive by its failure to account for the very close correspondence between factor-free accuracy, A_{nf}, and the y axis intercepts, F_2, in Fig. 5. From these arguments, in conjunction with Occam's razor, we prefer the simple mechanism in Fig. 1 to other and more complex alternatives.

Outlook: Are There also Two Proofreading Steps in Eukaryote Protein Synthesis? The present demonstration of two proofreading steps during mRNA translation on the bacterial ribosome resonates with recent cryo-EM data of translating ribosomes directly prepared from live human cells (20). Spahn and coworkers (20) identified a ribosome complex containing aa-tRNA in A/T state with eEF1α in the GDP conformation, where domains II and III were ordered, maintaining the interaction with the tRNA T-stem, while the G domain was disordered. This complex was about equally populated as a preaccommodation complex without eEF1α with aa-tRNA in similar position. These complexes were proposed to constitute two proofreading states from which the near-cognate tRNA can be rejected. This proposition is strongly supported by the present data, and we suggest that, in the living eukaryotic cell, ternary complexes of aa-tRNA·eEF1α·GDP may either dissociate from the ribosome in a first proofreading step or allow the aa-tRNA to move forward by release of eEF1α·GDP to a second proofreading step, only involving aa-tRNA. Together with the present findings, this suggests two-step proofreading mechanisms to be at work in bacteria, in the eukaryotes, and, by speculative inference, in all three kingdoms of life.

Can One GTP Molecule Drive Two Proofreading Steps? One may ask if the obligatory thermodynamic force that drives the exit reactions of substrates in proofreading (5, 6) is sufficient to drive the two proofreading steps suggested in the present work (Fig. 1). An upper limit of accuracy enhancement of the type of proofreading described here is given by the shift of GTP above equilibrium with its hydrolytic product, estimated as 10^9 to 10^{10} (5). This limit demonstrates the feasibility of a multistep accuracy enhancement in the range of 10^6, far above the here observed modest accuracy amplification in the range of 300. In more concrete terms, the two proofreading steps are separated by dissociation of EF-Tu·GDP, which is virtually irreversible due to rapid, EF-Ts–catalyzed conversion of EF-Tu·GDP to EF-Tu·GTP followed by ternary complex formation (28–30). Furthermore, there is no negative interference in the second proofreading step by a significant influx of free aa-tRNA, because the efficiency of ribosome binding is orders of magnitude smaller for free in relation to EF-Tu–bound aa-tRNA, and the major aa-tRNA fraction off the ribosome is EF-Tu–bound.

Why Did Mother Nature Evolve Two Proofreading Steps in Genetic Code Translation? The existence of two distinct proofreading steps may appear surprising, because the accuracy of initial codon selection by ternary complex normally is remarkably high (22, 31). Therefore, we suggest that two-step proofreading has evolved to neutralize the deleterious effects of a small number of distinct error hot spots for initial codon selection (31) as observed in vitro (19) and in vivo (18). For instance, initial codon selection values near 100 were seen for Glu-tRNA$^{Glu}_{UUC}$ reading GGA and His-tRNA$^{His}_{GUG}$ reading CGC (31). At high initial selection values (I), log$F$ decreases linearly with log$I$ with a slope close to 2, but as log$I$ decreases further at low I values, log$F$ remains virtually constant (19). This behavior is readily accounted for by the existence of two proofreading steps, where, in the high accuracy range, the amplification factors F_1 and F_2 decrease in proportion to decreasing maximal possible single-step accuracies d_{F1} and d_{F2}, respectively (see *SI Three-Step Codon Selection*). In the low accuracy range, in contrast, F_1 and F_2 remain approximately constant at further decrease in d_{F1} and d_{F2} by compensating increase in the corresponding ratios between discard and forward rate constants (a values) in each step (19); $a_{F1} = q_1/k_{Tu}$ for the first proofreading step, and $a_{F2} = q_2/k_{pep}$ for the second proofreading step (Fig. 1 and *SI Three-Step Codon Selection*). Such accuracy compensation by proofreading is only possible at a_{F1} and a_{F2} values much smaller than 1, as made feasible by multistep proofreading (5).

Proofreading and the Accuracy of Factor-Free Codon Selection. We have found, for the data set in Fig. 5, that the accuracy, A_{nf}, of factor-free codon selection is indistinguishable from the accuracy amplification conferred by the second proofreading step, F_2, of factor-dependent codon selection. This similarity is highlighted by the average of the F_2/A_{nf} ratios over the six cases in Fig. 5 that we estimate as 0.98 ± 0.08. The reason for this similarity is, we suggest, that, when the first proofreading selection ends by dissociation of EF-Tu·GDP from the ribosome, aa-tRNA is in a ribosome-bound high standard free energy complex from which it may be discarded or rapidly accommodated in the A site. In fact, this very scenario may be played out in the previously mentioned cryo-EM snapshot from human cells (see figure 1C in ref. 20). Furthermore, during factor-free

aa-tRNA binding to the posttranslocation ribosome (Scheme S1), aa-tRNA-entry into the A site requires passage through the very same complex of high standard free energy as the one rapidly reached with the help of EF-Tu and GTP hydrolysis in factor-dependent A-site binding (A/T state). A scenario, which leads to the virtually identical A_{nf} and F_2 values seen in Fig. 5, is described in *SI Factor-Free Codon Selection by aa-tRNA*. Further study of the strong correlation between A_{nf} and F_2 is important for three reasons. The first reason is that, when A_{nf} and F_2 are equal, there is no room for two EF-Tu–dependent proofreading steps where one depends on K_A and the other one does not. Secondly, in such cases, estimation of A_{nf} provides a shortcut to the determination of F_2 with very high precision. The third reason is that the aa-tRNA–ribosome complex in the metastate just after EF-Tu·GDP release can provide valuable information regarding the path by which aa-tRNA accommodates into the A site.

Another View of EF-Tu Function After Initial Selection. A different view of the role of EF-Tu after initial selection was recently proposed (32). From single-molecule and ensemble kinetics at 21 °C and 25 °C, respectively, in low-accuracy buffer (10), Liu et al. (32) concluded that, after GTP hydrolysis on EF-Tu (Fig. 1), the ribosome forms a complex (Complex B of Liu et al.) with EF-Tu still in the GDP form bound to L11 [scheme 1 of Liu et al.]. After release of Pi and separation of EF-Tu from L11, A-site accommodation of aa-tRNA and peptidyl transfer with EF-Tu in the GTP form take place [Complex C of Liu et al. (32)]. Then, EF-Tu switches to the GDP form and leaves the ribosome. Here, the main role of EF-Tu is to promote rapid A-site accommodation of aa-tRNA. From their buffer and temperature choices, we infer that proofreading (Fig. 5) and initial selection (31) are greatly reduced compared with in vivo rate (26, 33) and accuracy (19) calibrated systems. Comparison of our data sets is therefore nontrivial. At face value, we propose EF-Tu to rapidly change conformation after GTP hydrolysis and provide a second proofreading step, whereas Liu et al. (32) propose EF-Tu in the GTP form to promote rapid aa-tRNA accommodation followed by peptidyl transfer before conformational change and dissociation from the ribosome of the factor. It would, we think, be rewarding to combine their fluorescence-based single-molecule and ensemble kinetics and our quench-flow kinetics in experiments performed under similar conditions in an attempt to integrate our views on the function of EF-Tu after initial selection.

Consequences of the Present Findings. Apart from the unexpected finding of two proofreading steps, the present study has identified the structural basis of the first, EF-Tu–dependent, step and suggested mechanistic features of both proofreading steps. These findings will facilitate structural analysis of the proofreading steps along with structure-based computations of their codon-discriminating standard free energies for a deeper understanding of the evolution of accurate reading of the genetic code.

Materials and Methods

All experiments were performed at 37 °C in polymix buffer (34) with varying Mg^{2+} concentration. For cognate and near-cognate GTP hydrolysis measurements, ribosomes (1 μM) were in excess over ternary complexes (0.5 μM); both mixtures were prepared as described in ref. 31. For EF-Tu–dependent dipeptide formation measurements, ternary complexes (0.5 μM to 2 μM) were in excess over ribosomes (0.2 μM). For factor-free dipeptide formation measurements, EF-Tu and EF-Ts were omitted from the reactions, aa-tRNAs (1 μM to 6 μM) were in excess over ribosomes (0.2 μM) (see *SI Materials and Methods*).

ACKNOWLEDGMENTS. We thank J. Wang and J. Zhang for technical advice and J. Puglisi and M. Johansson for comments on the manuscript. This work was supported by grants from the Knut and Alice Wallenberg Foundation to the Ribosome Consortium of Research and Education (RiboCORE), the Swedish Research Council, and the Human Frontier Science Program.

1. Pauling L (1957) The probability of errors in the process of synthesis of protein molecules. *Festschrift Arthur Stoll*, ed Birkhauser A (Birkhauser, Basel), pp 597–602.
2. Loftfield RB, Vanderjagt D (1972) The frequency of errors in protein biosynthesis. *Biochem J* 128(5):1353–1356.
3. Hopfield JJ (1974) Kinetic proofreading: A new mechanism for reducing errors in biosynthetic processes requiring high specificity. *Proc Natl Acad Sci USA* 71(10):4135–4139.
4. Ninio J (1975) Kinetic amplification of enzyme discrimination. *Biochimie* 57(5):587–595.
5. Ehrenberg M, Blomberg C (1980) Thermodynamic constraints on kinetic proofreading in biosynthetic pathways. *Biophys J* 31(3):333–358.
6. Kurland CG (1978) The role of guanine nucleotides in protein biosynthesis. *Biophys J* 22(3):373–392.
7. Hopfield JJ, Yamane T, Yue V, Coutts SM (1976) Direct experimental evidence for kinetic proofreading in amino acylation of tRNAIle. *Proc Natl Acad Sci USA* 73(4):1164–1168.
8. Ruusala T, Ehrenberg M, Kurland CG (1982) Is there proofreading during polypeptide synthesis? *EMBO J* 1(6):741–745.
9. Thompson RC, Stone PJ (1977) Proofreading of the codon–anticodon interaction on ribosomes. *Proc Natl Acad Sci USA* 74(1):198–202.
10. Gromadski KB, Rodnina MV (2004) Kinetic determinants of high-fidelity tRNA discrimination on the ribosome. *Mol Cell* 13(2):191–200.
11. Zaher HS, Green R (2010) Hyperaccurate and error-prone ribosomes exploit distinct mechanisms during tRNA selection. *Mol Cell* 39(1):110–120.
12. Johansson M, Lovmar M, Ehrenberg M (2008) Rate and accuracy of bacterial protein synthesis revisited. *Curr Opin Microbiol* 11(2):141–147.
13. Demeshkina N, Jenner L, Westhof E, Yusupov M, Yusupova G (2012) A new understanding of the decoding principle on the ribosome. *Nature* 484(7393):256–259.
14. Freter RR, Savageau MA (1980) Proofreading systems of multiple stages for improved accuracy of biological discrimination. *J Theor Biol* 85(1):99–123.
15. Murugan A, Huse DA, Leibler S (2012) Speed, dissipation, and error in kinetic proofreading. *Proc Natl Acad Sci USA* 109(30):12034–12039.
16. Maracci C, Rodnina MV (2016) Review: Translational GTPases. *Biopolymers* 105(8):463–475.
17. Rodnina MV, Wintermeyer W (2016) Protein elongation, co-translational folding and targeting. *J Mol Biol* 428(10 Pt B):2165–2185.
18. Manickam N, Nag N, Abbasi A, Patel K, Farabaugh PJ (2014) Studies of translational misreading in vivo show that the ribosome very efficiently discriminates against most potential errors. *RNA* 20(1):9–15.
19. Zhang J, Ieong KW, Mellenius H, Ehrenberg M (2016) Proofreading neutralizes potential error hotspots in genetic code translation by transfer RNAs. *RNA* 22(6):896–904.
20. Behrmann E, et al. (2015) Structural snapshots of actively translating human ribosomes. *Cell* 161(4):845–857.
21. Vorstenbosch E, Pape T, Rodnina MV, Kraal B, Wintermeyer W (1996) The G222D mutation in elongation factor Tu inhibits the codon-induced conformational changes leading to GTPase activation on the ribosome. *EMBO J* 15(23):6766–6774.
22. Johansson M, Zhang J, Ehrenberg M (2012) Genetic code translation displays a linear trade-off between efficiency and accuracy of tRNA selection. *Proc Natl Acad Sci USA* 109(1):131–136.
23. Schrader JM, Chapman SJ, Uhlenbeck OC (2011) Tuning the affinity of aminoacyl-tRNA to elongation factor Tu for optimal decoding. *Proc Natl Acad Sci USA* 108(13):5215–5220.
24. Schrader JM, Chapman SJ, Uhlenbeck OC (2009) Understanding the sequence specificity of tRNA binding to elongation factor Tu using tRNA mutagenesis. *J Mol Biol* 386(5):1255–1264.
25. Ieong KW, Pavlov MY, Kwiatkowski M, Forster AC, Ehrenberg M (2012) Inefficient delivery but fast peptide bond formation of unnatural L-aminoacyl-tRNAs in translation. *J Am Chem Soc* 134(43):17955–17962.
26. Johansson M, Bouakaz E, Lovmar M, Ehrenberg M (2008) The kinetics of ribosomal peptidyl transfer revisited. *Mol Cell* 30(5):589–598.
27. Asahara H, Uhlenbeck OC (2002) The tRNA specificity of *Thermus thermophilus* EF-Tu. *Proc Natl Acad Sci USA* 99(6):3499–3504.
28. Burnett BJ, et al. (2013) Elongation factor Ts directly facilitates the formation and disassembly of the *Escherichia coli* elongation factor Tu·GTP·aminoacyl-tRNA ternary complex. *J Biol Chem* 288(19):13917–13928.
29. Gromadski KB, Wieden HJ, Rodnina MV (2002) Kinetic mechanism of elongation factor Ts-catalyzed nucleotide exchange in elongation factor Tu. *Biochemistry* 41(1):162–169.
30. Ruusala T, Ehrenberg M, Kurland CG (1982) Catalytic effects of elongation factor Ts on polypeptide synthesis. *EMBO J* 1(1):75–78.
31. Zhang J, Ieong KW, Johansson M, Ehrenberg M (2015) Accuracy of initial codon selection by aminoacyl-tRNAs on the mRNA-programmed bacterial ribosome. *Proc Natl Acad Sci USA* 112(31):9602–9607.
32. Liu W, et al. (2015) EF-Tu dynamics during pre-translocation complex formation: EF-Tu·GDP exits the ribosome via two different pathways. *Nucleic Acids Res* 43(19):9519–9528.
33. Borg A, Ehrenberg M (2015) Determinants of the rate of mRNA translocation in bacterial protein synthesis. *J Mol Biol* 427(9):1835–1847.
34. Jelenc PC, Kurland CG (1979) Nucleoside triphosphate regeneration decreases the frequency of translation errors. *Proc Natl Acad Sci USA* 76(7):3174–3178.
35. Polekhina G, et al. (1996) Helix unwinding in the effector region of elongation factor EF-Tu-GDP. *Structure* 4(10):1141–1151.
36. Voorhees RM, Schmeing TM, Kelley AC, Ramakrishnan V (2010) The mechanism for activation of GTP hydrolysis on the ribosome. *Science* 330(6005):835–838.
37. Jones TA, Zou JY, Cowan SW, Kjeldgaard M (1991) Improved methods for building protein models in electron density maps and the location of errors in these models. *Acta Crystallogr A* 47(Pt 2):110–119.
38. Wold F, Ballou CE (1957) Studies on the enzyme enolase. I. Equilibrium studies. *J Biol Chem* 227(1):301–312.
39. Johansson M, et al. (2011) pH-sensitivity of the ribosomal peptidyl transfer reaction dependent on the identity of the A-site aminoacyl-tRNA. *Proc Natl Acad Sci USA* 108(1):79–84.
40. Gromadski KB, Daviter T, Rodnina MV (2006) A uniform response to mismatches in codon-anticodon complexes ensures ribosomal fidelity. *Mol Cell* 21(3):369–377.